J. Geogr. Sci. 2022, 32(11): 2349-2364
DOI: https://doi.org/10.1007/s11442-022-2051-0

Baseline determination, pollution source and ecological risk of heavy metals in surface sediments of the Amu Darya Basin, Central Asia

ZHAN Shuie[1,2], *WU Jinglu[1,2], JIN Miao[1,2], ZHANG Hongliang[1,2]

1. State Key Laboratory of Lake Science and Environment, Nanjing Institute of Geography and Limnology, CAS, Nanjing 210008, China;
2. University of Chinese Academy of Sciences, Beijing 100049, China

Abstract: Central Asia (CA) is one of the most fragile regions worldwide owing to arid climate and accumulated human activities, and is a global hotspot due to gradually deteriorating ecological environment. The Amu Darya Basin (ADB), as the most economically and demographically important region in CA, is of particular concern. To determine the concentration, source and pollution status of heavy metals (HMs) in surface sediments of the ADB, 154 samples were collected and analyzed for metals across the basin. Correlation and cluster analysis, and positive matrix factorization model were implemented to understand metals' association and apportion their possible sources. Cumulative frequency distribution and normalization methods were used to determine the geochemical baseline values (GBVs). Then, various pollution indices and ecological risk index were employed to characterize and evaluate the pollution levels and associated risks based on the GBVs. Results indicated that the mean concentrations of HMs showed the following descending order in the surface sediments of ADB: Zn > Cr > Ni > Cu > Pb > Co > Cd. The spatial distribution maps showed that Cr, Ni, and Cu had relatively high enrichment in the irrigated agricultural area; high abundances of Zn, Pb, and Cd were mainly found in the urban areas. Four source factors were identified for these metals, namely natural sources, industrial discharge, agricultural activities, and mixed source of traffic and mining activities, accounting for 33.5%, 11.4%, 34.2%, and 20.9% of the total contribution, respectively. The GBVs of Cd, Zn, Pb, Cu, Ni, Cr, and Co in the ADB were 0.27, 58.9, 14.6, 20.3, 25.8, 53.4, and 9.80 mg/kg, respectively, which were similar to the regional background values obtained from lake sediments in the bottom. In general, the assessment results revealed that surface sediments of the ADB were moderately polluted and low ecological risk by HMs.

Keywords: heavy metal; spatial distribution; source identification; geochemical baseline value; risk assessment; Amu Darya Basin

Received: 2022-01-05 **Accepted:** 2022-06-09

Foundation: Strategic Priority Research Program of Chinese Academy of Sciences, Pan-Third Pole Environment Study for a Green Silk Road, No.XDA2006030101; National Natural Science Foundation of China, No.U2003202

Author: Zhan Shuie (1986–), PhD Candidate, specialized in environmental geochemistry of lakes. E-mail: zhanshuie@126.com

*Corresponding author: Wu Jinglu, Professor, E-mail: w.jinglu@niglas.ac.cn

1 Introduction

Central Asia (CA), located in the hinterland of Eurasian continent, is of geopolitical and strategic importance. CA countries usually consists of five former Soviet Union countries, with a population of over 75 million by 2020 (The World Bank, 2021). Large part of CA has a semi-arid to arid climate, characterized by scarce precipitation and high evaporation, which is one of the most fragile ecosystems in the world (Jiang *et al*., 2019; Zhang *et al*., 2019). Despite the abundance of mineral resources to meet energy needs, irrigated agriculture remains the main economic backbone of most CA countries (Hamidov *et al*., 2016). Water resources are therefore a critical factor limiting economic development in CA (Mueller *et al*., 2014; Shen *et al*., 2021; Zhan *et al*., 2022). However, the environmental problems in water and sediments caused by the population growth, industrial and agricultural activity strengthened in this region in recent decades are becoming increasingly prominent (Awan *et al*., 2011; Karthe *et al*., 2015; Hu *et al*., 2018).

As the most important river in CA, the environmental aspects of the Amu Darya have always been the focus of research (Ataniyazova, 2003; Crosa *et al*., 2006; Ma *et al*., 2020; Zhan *et al*., 2022). The Amu Darya Basin (ADB), covering several countries, including most of Tajikistan, Afghanistan, and Uzbekistan as well as small of Turkmenistan and Kyrgyzstan, supplies most of their water and other energy resources (Babow and Meisen, 2012). However, under the combined effects of arid climate and aggravated human activities caused by large-scale development of irrigated agriculture and mismanagement of resources, the ecological environment of the ADB has gradually deteriorated and triggered ecological crises (Micklin, 2007; Sun *et al*., 2019). Most worryingly, high levels of heavy metals (HMs), organic pollutants and other toxic substances were detected in the blood of pregnant women and children in the lower ADB, and a series of health problems such as high infant mortality, low birth weight, growth retardation, acute respiratory diseases, diarrheal diseases and other diseases were observed in the area (Ataniyazova *et al*., 2001; Kaneko *et al*., 2003). To date, however, the concentration status and sources of pollutants in the environment throughout the ADB are not clear, which creates great uncertainty for local pollution control and prevention.

Exploring the properties of HMs in sediments can provide clues of anthropogenic effects and identify pollutant source (Kodirov *et al*., 2018; Liao *et al*., 2019; Ramazanova *et al*., 2021; Xiao *et al*., 2021). Through the analysis of HMs in sediments, Zhang *et al*. (2021) concluded that in addition to human activities, natural sources of HMs in the Yarlung Tsangpo River basin cannot be ignored; Yang *et al*. (2021) found that HM concentrations in sediments of karstic environments in Guangxi were primarily influenced by the natural geological background. Lepeltier (1969) have determined the geological baselines by cumulative frequency distribution (CDF) to distinguish the natural sources of HMs from other possible sources in the environmental media. Some studies also conducted HM pollution assessment by establishing regional geochemical baseline values (GBVs) to reveal the origins of pollution and the impact of human activities (Jiang *et al*., 2021; Magesh *et al*., 2021). In this study, we determined GBVs for HMs in surface sediments from the entire ADB via a combination of CDF method by normalization method. The present study aims (1) to analyze the concentrations and spatial variation characteristics of HMs in the surface sediments; (2) to quantitatively identify the potential sources of HMs; (3) to assess the pollution levels

and potential ecological risk of HMs in surface sediments based on the establishing regional GBVs. Therefore, this study was designed to provide an insight into the levels and sources of the HM pollution in surface sediments from the ADB, which could serve as a reference for subsequent studies.

2 Materials and methods

2.1 Study area

The ADB, located between 34°30′N–43°45′N and 58°15′E–75°07′E, is an essential region for the construction of the Belt and Road (Figure 1). It covers a drainage area of 465,000 km^2, of which approximately 200,000 km^2 are in the highest mountainous areas of the Pamir Mountains (Wang *et al*., 2016). The basin is critical to the economy and livelihoods of most of the CA population, housing more than 50 million people (Babow and Meisen, 2012; Salehie *et al*., 2021). The climate changes drastically according to elevation in ADB, and most of the basin is continental, with dry and hot summer and bitterly cold winter. Average annual precipitation is over 1000 mm in the high mountain areas. However, in the plain areas of the lower ADB, the average annual precipitation is only 100 mm, and evaporation is up to 1150 mm (Awan *et al*., 2011; Sun *et al*., 2019). Due to the diversity of geography and the uneven distribution of resources, production activities differ greatly among the countries within the watershed. Countries located in plain areas are rich in arable land resources, and irrigated agriculture occupies an important role. Uzbekistan, for example, has

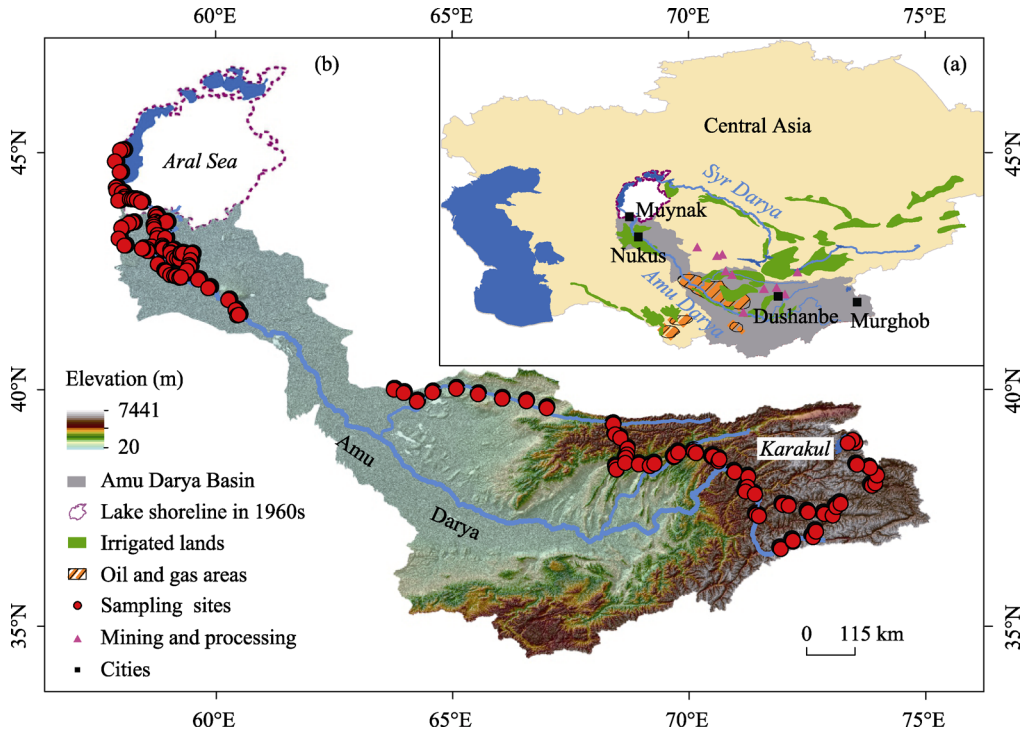

Figure 1 Location of the study area and sample sites (a. Geographical location of the Amu Darya Basin (ADB) (based on maps from: www.cawater-info.net/infographic/index_e.htm); b. sampling locations along the ADB)

10.7 million ha of cultivated land and is highly developed in irrigated agriculture (Brody *et al*., 2020). Whereas, for mountainous countries, cultivated land is very scarce, but rich in water and mineral resources. Consequently, although agriculture remained the main source of economy, the contribution of the mining industry could not be ignored, as in Tajikistan, where it accounted for 30% of the country's economy (Central Asian Geoportal). In recent decades, with the exploitation of the mineral resources and the development of industry and agriculture, the pollutants released into the environment have increased, which has aroused wide public concern (Skipperud *et al*., 2013; Shukurov *et al*., 2014).

2.2 Sample collection and laboratory analyses

A total of 154 surface sediment (0–5 cm) samples were collected from the ADB. Sampling in the upper watershed in Tajikistan (samples S88–S154) was completed in October 2011 and in the middle and lower watershed within Uzbekistan (samples S1–S87) in August 2019. Due to the wide extent and topographic complexity of the study area, sample collection was primarily based on accessibility and ensuring the representation of different types of surface sediments. So, some samples in high mountainous areas were collected in the city of Dushanbe as well as along roads. The locations of the sampling sites were determined using a portable GPS (Table S1). Each sample was placed in a clean polyethylene bag and marked with the sample information on the bag. Samples were transported to the laboratory and immediately dried at –50 ℃ for 48 hours using a vacuum freeze dryer (Xiao *et al*., 2021). The dried samples were then ground using an agate mortar and pestle, and then filtered through a 200-mesh sieve to obtain a powdered precipitate for each sample (Zhan *et al*., 2020).

Inductively coupled plasma mass spectrometry (ICP-MS, Agilent Technologies 7700, USA) was used to measure the concentrations of the metals. The detection limits for these metals were Ca (5 mg/kg), Mg (2 mg/kg), Na (20 mg/kg), Al (20 mg/kg), Ti (1 mg/kg), Fe (5 mg/kg), Zn (2 mg/kg), Pb (0.02 mg /kg), Ni (0.05 mg/kg), Cr (0.1 mg/kg), Cu (0.02 mg/kg), Cd (0.01 mg/kg) and Co (0.01 mg/kg). Reagent blanks were performed alongside sample analyses to ensure the analytical quality. All the values for tested blanks were below 5% of the sample values. Recoveries between the measured values and standard solution were in the range of 91.6%–105.3%. The relative standard deviations (RSD) of the replicates were all within 10%.

2.3 Positive matrix factorization model

Positive matrix factorization model (PMF) is an effective multivariate factor analysis tool for identifying pollution sources (Paatero and Tapper, 1994; Chai *et al*., 2021). In this study, EPA PMF 5.0 was used to quantify the various sources of metals in surface sediment samples. The model is a decomposition of the original matrix x into three matrices: the factor scores matrix (g), the factor loading matrix (f) and the residual matrix (e). The equation was as follows:

$$x_{ij} = \sum_{k=1}^{p} g_{ik} f_{kj} + e_{ij} \tag{1}$$

where x_{ij} represents the concentration of HM j in the ith sample; g_{ik} represents the source contribution of k in the ith sample; f_{kj} represents the amount of HM j from source k; and e_{ij} is residual error obtained by minimizing the objective function Q:

$$Q = \sum_{i=1}^{n} \sum_{j=1}^{m} \left[\frac{x_{ij} - \sum_{k=1}^{p} g_{ik} f_{kj}}{u_{ij}} \right]^2 \tag{2}$$

Here, u_{ij} is the uncertainty of HM j in the ith sample, calculated as follows:

$$\text{if } c \le \text{MDL}, u_{ij} = 5/6 \times MDL \tag{3}$$

$$\text{otherwise}, u_{ij} = \sqrt{(errorfraction \times c)^2 + MDL^2} \tag{4}$$

where the *errorfraction* represents the RSD, C represents the concentration of HM, and *MDL* represents the method detection limit.

2.4 Establishment of regional geochemical baseline

The regional GBVs for HMs in the ADB was established using cumulative frequency curves and normalization methods. For the cumulative frequency curves method, GBV for each HMs was determined by plotting CFD curves, where the cumulative frequencies were displayed on the X-axis and the metal concentrations or transformed values of concentrations were displayed on the Y-axis (Lepeltier, 1969). Prior to plotting the CFD curves, a Kolmogorov-Smirnov (K-S) test should be carried out to confirm the normality of the elemental distribution (Karim *et al*., 2015). The CFD inflection was identified under a linear regression model with $p < 0.05$ and $R^2 > 0.9$, and the outliers were excluded until the remaining values met this criterion (Wei and Wen, 2012). The inflection point split the graph into a front part (low concentrations) and a back part (high concentrations) (Figure S1); the front part was supposed to have a geological source, while the back part was considered to have anthropogenic sources, or other biological sources (Jiang *et al*., 2021). Ultimately, the GBV was obtained by averaging the data from the front part of the inflection point. For the normalization method, the inert element Al was chosen as the normalizer to exclude the effect of grain size (Zeng *et al*., 2014). A linear regression equation was firstly built between each HM and Al as follows:

$$C_{HM} = aC_{Al} + b \tag{5}$$

where C_{HM} and C_{Al} represent the concentrations of HM and Al, respectively; a and b are regression constants. In equation (5), natural sediments were determined by points that fell within the 95% confidence interval, while points falling outside the confidence interval were considered to reflect anthropogenic inputs (Zhou *et al*., 2021). The GBV were therefore calculated by data points that fell within the 95% confidence interval using the following equation:

$$GBV_{HM} = c\overline{C}_{Al} + d \tag{6}$$

Here, $\overline{C}_{Al}$ is the mean concentration of Al at selected points; c and d are the redetermined regression constants between HM and Al.

2.5 Pollution assessment

Single-factor pollution index (*PI*) and pollution load index (*PLI*) were powerful tools for assessing HM contamination in sediments. Among them, *PI* reflected the contamination level of an individual HM. The *PLI* was a combined pollution index calculated from the *PI* of

all HMs. The *PI* and *PLI* were defined as follows (Tomlinson *et al*., 1980):

$$PI_i = \frac{C_i}{C_{GB}} \tag{7}$$

$$PLI = \sqrt[n]{PI_1 \times PI_2 \times PI_3 \times \cdots\cdots \times PI_n} \tag{8}$$

where C_i represents the measured HM concentration, and C_{GB} represents the GBV of the HM. Accordingly, HM pollution can be divided into different classifications, shown in Table S2.

The potential ecological risk index (*PERI*) was first introduced by Hakanson (Hakanson, 1980). This index is widely used to assess the potential ecological risk of HMs in the sediments. E^i_r reflected the ecological risk coefficient for individual HM. *PERI* was the comprehensive ecological risk factor calculated from the E^i_r of all HMs. The E^i_r and *PERI* were defined as follows:

$$E^i_r = T^i_r \times C^i_s / C^i_n \tag{9}$$

$$PERI = \sum\nolimits_{n=1}^{n} E^i_r \tag{10}$$

Here, T^i_r represents the toxic-response factor (Zn = 1, Cd = 30, Co = Pb = Cu = 5; Cr = Ni = 2) (Hakanson, 1980); C^i_s represents the measured HM concentration; C^i_n represents the reference values of HM. The corresponding classification criteria were also shown in Table S2.

2.6 Statistical analyses

In this study, descriptive statistics were performed using Microsoft Excel 2016. Statistical analyses were conducted on the HMs using SPSS 25.0 software. CFD curves, clustering heat map and cumulative percentage map were plotted using Origin 2018 software. The spatial distributions of normalized metallic elements were mapped using ArcGIS 10.2. EPA PMF 5.0 was applied to analyze and quantify the main sources of elemental metals.

3 Results and discussion

3.1 Concentration variations of metallic elements

Descriptive statistical results of Ca, Mg, Na, Al, Ti, Fe, Cd, Zn, Pb, Cu, Ni, Cr and Co in surface sediment samples from the ADB were listed in Table 1. The concentrations of metals ranged widely and varied significantly between the sampling sites. The coefficients of variation (CV) for most of the metal concentrations exhibited high values except for Al (21.90%), Ti (30.34%), Fe (30.62%) and Co (31.77%), which indicated that the sediments in the ADB probably were affected by discrete inputs associated with anthropogenic activities or natural processes (Adimalla *et al*., 2020). The highest concentrations of Ca, Mg, Na, Al, Ti, Fe, Cd, Zn, Pb, Cu, Ni, Cr and Co were recorded at sample sites S5, S140, S90, S143, S107, S107, S94, S115, S20, S115, S95, S108, S115, respectively. The lowest concentration of Ca was found at S72, Mg, Ti, Fe, Cu, Ni, Cr and Co at S140, Na at S90, Al at S5, Cd at S141, Pb at S152, Zn at S121. Interestingly, the maximum concentrations of most metallic elements were observed in the mountainous area, primarily located near the city of Dushanbe (such as S90 and S94) and the roadside (such as S108), while the minimum concentrations of most elements were also found in mountainous areas, mainly in remote areas that were less affected by human activities (such as S140, S141 and S152). In addition, the average concen-

trations of all HMs (Cd, Zn, Pb, Cu, Ni and Cr) exceeded their median values except for Co, suggesting unusually high HM concentrations at some sample sites in the study area.

Table 1 Statistics of elemental concentrations in the surface sediments of the Amu Darya Basin and data on metal concentrations from other study areas

Metals	ADB[1] (N=154)						CSR[2]	IKLR[3]	CA[4]	BMV[5]
	Max	Min	Ave.	Median	SD	CV (%)	Ave.	Ave.	Ave.	Median
Ca (mg/g)	172.2	10.16	68.00	69.44	32.84	48.29	126	—	—	15
Mg (mg/g)	46.29	1.87	16.52	16.47	6.20	37.50	10.4	—	—	5
Na (mg/g)	175.3	5.24	18.18	14.39	17.24	94.86	—	—	—	5
Al (mg/g)	80.67	19.04	54.46	56.07	11.93	21.90	39	—	—	71
Ti (mg/g)	8.65	0.37	2.89	2.96	0.88	30.43	—	—	—	5
Fe (mg/g)	61.45	3.56	27.26	27.77	8.34	30.62	20	31.86	—	40
Cd (mg/kg)	1.81	0.04	0.36	0.27	0.30	82.55	0.1	0.17	0.43	0.35
Zn (mg/kg)	210.4	20.87	68.73	65.03	29.12	42.36	46.0	77.39	67.40	9
Pb (mg/kg)	52.84	3.28	18.61	15.50	8.71	46.83	11.3	23.92	19.84	35
Cu (mg/kg)	142.8	1.81	23.78	22.53	15.76	66.27	19.5	16.37	22.87	30
Ni (mg/kg)	228.2	1.46	28.37	27.30	19.19	67.64	29.8	20.23	24.82	50
Cr (mg/kg)	384.1	2.88	59.67	58.14	34.11	57.17	56.1	45.78	58.97	70
Co (mg/kg)	22.56	2.40	10.40	10.62	3.30	31.77	8.8	9.55	10.52	8

[1] Amu Darya Basin; [2] Caspian Sea region (De Mora *et al*., 2004); [3] Issyk-Kul Lake region (Ma *et al*., 2018); [4] Central Asia (Wang *et al*., 2021a); [5] Worldwide (CNEMC, 1990)

Generally, the average/median concentrations of various metals showed the following descending order in the surface sediments of ADB: Ca > Al > Fe > Na > Mg > Ti > Zn > Cr > Ni > Cu > Pb > Co > Cd (Table 1). Among them, the median concentrations of Ca, Mg, Na, Zn and Co exceeded their corresponding background median values of sediments worldwide (BMVs), while the median concentrations of other metals were within their BMVs (CNEMC, 1990). Also, the average concentrations of HMs were compared with previous relevant studies for other regions in CA (Table 1). It was found that the HM concentrations in surface sediments of the ADB were close to those throughout the CA, except for Zn, Cu and Ni (Wang *et al*., 2021a). Compared to the surface samples from the Caspian Sea region (CSR) and Issyk-Kul Lake region (IKLR), however, the sediments in the ADB had the highest mean concentrations of Cd, Cu and Cr, especially Cd, while the topsoil in IKLR had the highest average concentrations of Pb and Zn, and the surface samples from the CSR had the relatively high abundance of Ni (De Mora *et al*., 2004; Ma *et al*., 2018). The concentration levels of HMs in various regions exhibited large regional differences, which probably were influenced by human activities and the geological environment (Karim *et al*., 2015; Zhou *et al*., 2021).

3.2 Normalization and spatial distributions of metals

Assessing the spatial distribution of metals in surface sediments can be a good way to determine positions with higher HM contents and provide evidence of anthropogenic impacts (Chen *et al*., 2019; Wang *et al*., 2021a; Yang *et al*., 2021). To reduce the influence of particle size, and better understand geochemical characteristics and anthropogenic inputs of met-

al elements, the spatial distribution of metal concentrations with normalized values were essential (Zeng *et al*., 2014; Zhou *et al*., 2021). In this study, the conservative reference element, Al was selected as the normalizer, because it had the lowest CV among the metals. High normalized values of Ca, Na and Mg were observed in the lakeside areas, including the Aral Sea and Karakul (Figures 2a–2c), suggesting that these metals tended to flocculate or were susceptible to evaporation (Prabakaran *et al*., 2019). As for Fe, Ti and Co, they were evenly distributed throughout the basin, with relative enrichment in the downstream plain areas as well as in the riparian and lakeshore areas in the mountains (Figures 2d–2f). Generally, Cu, Ni and Cr were similarly distributed, and relatively enriched in irrigated agricultural areas in addition to urban areas, with lower values recorded around Murghob. High normalized values of Cu, Ni and Cr concentrations were found in sample sites S20 and S119, S115 as well as S107 and S115, respectively (Figures 2g–2i). Whereas, high normalized values of Cd were observed at sample sites S93–S96, S102 and S107, which were mainly located near the industrial outfalls and roads in city of Dushanbe (Figure 2j). In addition, high values of Zn and Pb also occurred in Murghob (such as samples S145, S146, S148 and S149) and in Nukus (such as S58) (Figure 2k–l), which were significantly influenced by human activities such as traffic exhaust emissions (Zhan *et al*., 2020; Ramazanova *et al*., 2021).

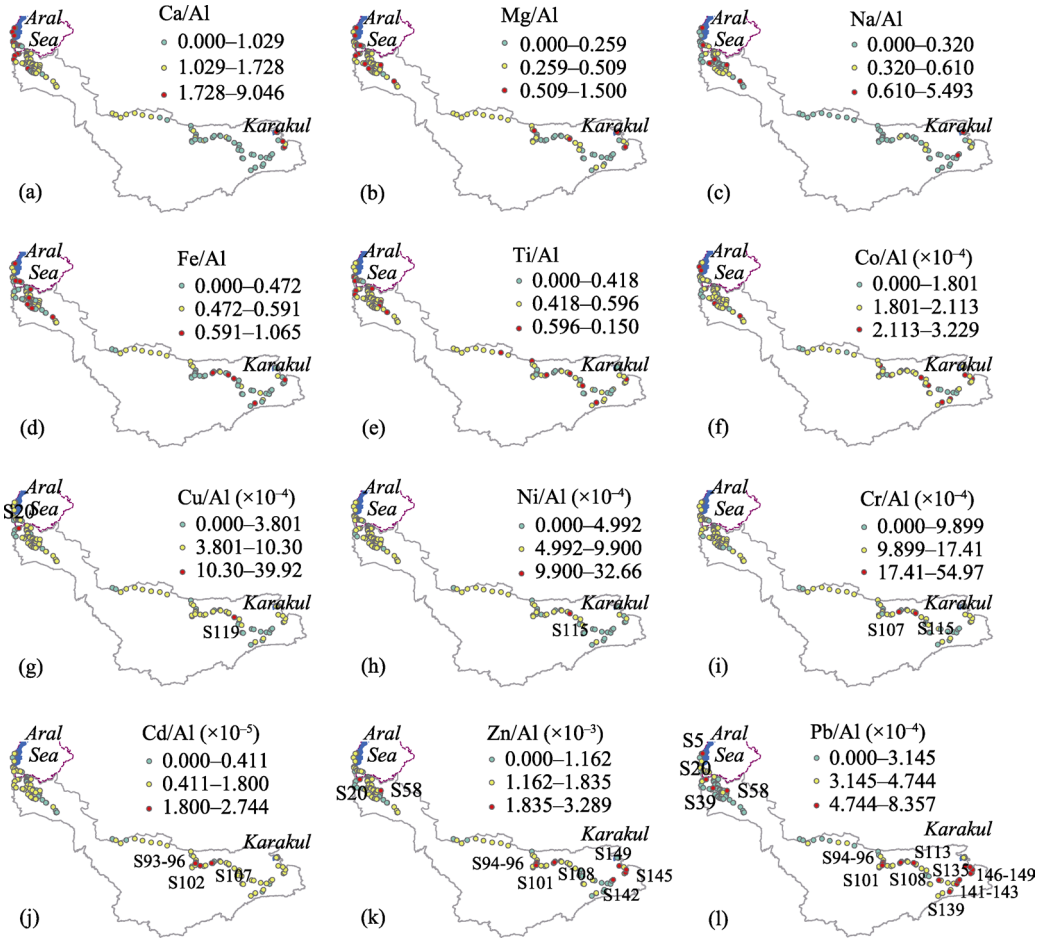

Figure 2 Spatial distribution of normalized metal concentrations in surface sediments of the Amu Darya Basin

3.3 Source apportionment

3.3.1 Correlation and cluster analysis

To understand whether the sources of the metals were consistent, correlation and cluster analysis were carried out on 15 metals in surface sediments of the ADB. As shown in Figure 3, the metals were divided into two groups. Moreover, a negative correlation or weak correlation between the elements in two groups indicates their different sources. Group 1 represented easily migratory elements, containing Ca, Mg and Na, which were characterized by having active chemical behavior and could be released from the silicate lattice at the initial stage of weathering and then taken with the water (Yang *et al*., 2021; Zhang *et al*., 2021). High enrichments of Ca, Mg and Na were observed in sediments from the lower ADB and lakeshore areas (Figure 2), which suffered from sparse precipitation and strong evaporation (Awan *et al*., 2011). Therefore, group 1 was probably related to the migration and flocculation of chemical elements in sediments as well as the strong evaporation caused by the arid climate. Group 2 contained elements that were very stable in the crust (Al, Fe and Ti) and seven HMs (Co, Cr, Ni, Cu, Pb, Zn and Cd). For the group 2 metals, Al, Fe Co and Ti were strongly correlated with each other, with Fe-Co showing the highest correlation (0.94), indicating that these metals might have the similar origins. In addition, Cr had a highly correlation with Ni (0.93), showing that they probably had the same source. There was also a strong

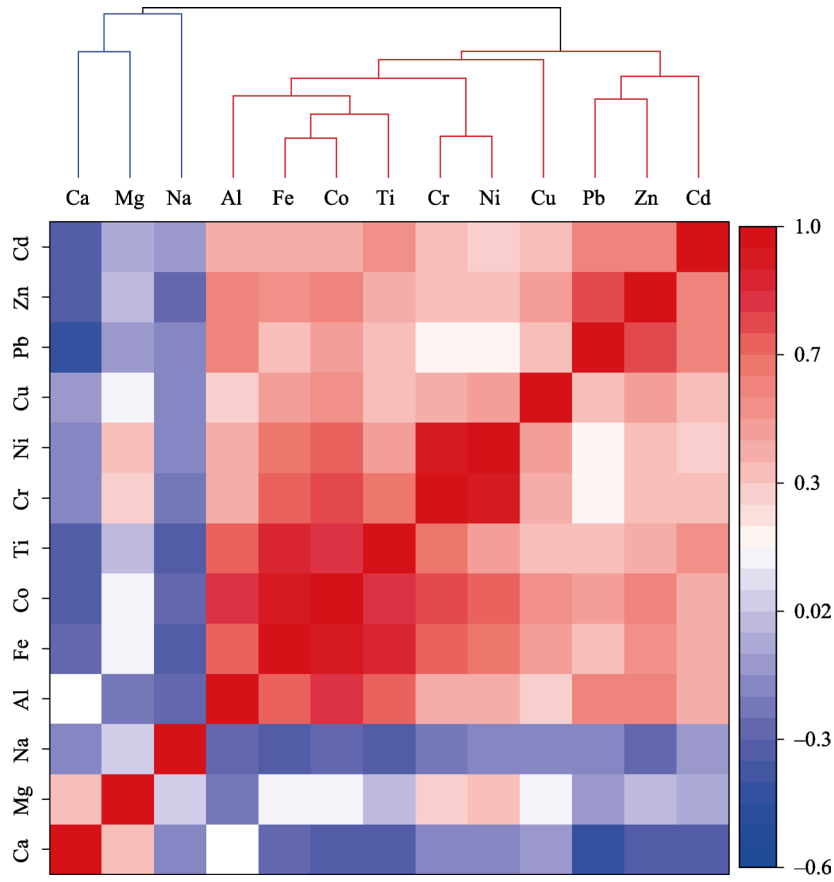

Figure 3 Clustering heat map between metallic elements

positive correlation between Zn and Pb (0.75), which was similar to the results of previous studies (Hossain *et al*., 2015). Cu showed moderate positive correlations with Cr and Ni and Cd with Pb and Zn, respectively, indicating that Cu was of similar origins to Cr and Ni and Cd to Pb and Zn. Spatially, Cr, Ni, Cu, Pb, Zn and Cd were primarily enriched in urban as well as agricultural areas and might be heavily influenced by human activities, while Al, Ti, Co and Fe were evenly distributed in the study area and were possibly derived from natural sources (Adimalla *et al*., 2020; Yang *et al*., 2021).

3.3.2 Quantitative source by PMF

In order to further assess the anthropogenic and natural sources of metal elements in the sediments, in this study, PMF model was used to quantitatively analyze the sources and contributions of 10 metals in group 2, which were relatively stable in their chemical behavior. The number of factors was set to 3, 4 and 5, respectively, and the model was run 20 times to find the minimum and stable Q value. When the number of factors was 4, the difference between Q_{robust} and Q_{true} was the smallest, and most of the residual were between –3 and 3, and the fitting coefficients R^2 between the observed and predicted values of the HMs ranged from 0.85 to 0.99, indicating that the results were reliable (Wang *et al*., 2020). Four factors were produced by PMF, as presented in Figure 4.

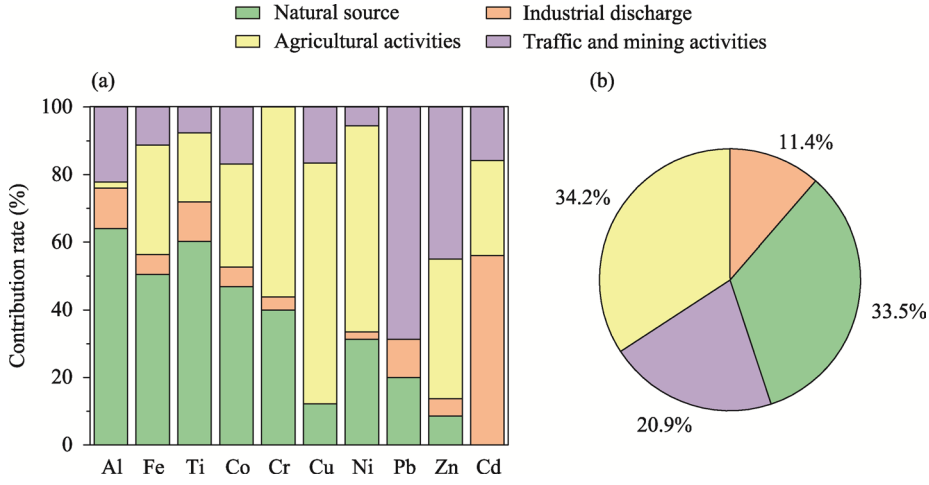

Figure 4 Source composition profiles of metals obtained using the PMF model (a) and percent contribution of each source to the metals in surface sediments of the Amu Darya Basin (b)

The first factor (F1) had higher relative contributions for Al (64.0%), Fe (50.5%), Ti (60.3%) and Co (46.9%) in the sediments of ADB, accounting for 33.5% of the total source contribution (Figure 4). In most environments, Al, Ti, Fe and Co were fairly stable and rarely occurred migration. These metals were probably from the parent rocks, or secondary enrichment during weathering (Taylor, 1964; Yang *et al*., 2021). In addition, Al, Ti, Fe and Co in our study also exhibited low CVs and more even spatial distribution, indicating that they were less influenced by the environment (Table 1 and Figure 2). Thus, F1 could be considered as a natural source connected to the parent rocks.

The second factor (F2) explained 11.4% of the total variance, which was characterized by Cd (56.1%). The highest CV (85.15%) was observed for Cd among the HMs, indicating that

anthropogenic sources were the dominant contribution to Cd contamination. Previous studies had revealed that Cd might come from electroplating industries, fossil fuel combustion and petroleum refining (Gunawardena *et al*., 2014; Jiang *et al*., 2021). Spatially, high enrichment of Cd occurred mainly near the industrial sewage outfalls (S94 and S95), roads (S93, S96), and riverbed sediments (S107) in the city of Dushanbe. Therefore, F2 could be identified as a possible source from industrial activities.

The third factor (F3) was predominated by Cr (56.2%), Cu (71.2%), Ni (60.9%) and Zn (41.3%), which accounted for 34.2% of the total contribution. Studies have found that Cu and its compounds were commonly associated with agricultural activities, which were usually added to insecticides and fungicides and found in livestock manure (Luo *et al*., 2009; Wu *et al*., 2021). Also, higher concentrations of Cr, Ni and Zn suggested anthropogenic sources such as the use of fertilizers and pesticides (Chen *et al*., 2019; Xiao *et al*., 2021). The high accumulation of Cu was exhibited in agricultural areas of the study area, such as samples S20 and S119 (Figure 2). Thus, F3 could be regarded as an agricultural source.

For the fourth factor (F4), Pb (68.7%) and Zn (44.9%) were the main loading elements, accounting for 20.9% of the contribution. It was shown that vehicle exhaust played a major role in Pb enrichment (Chai *et al*., 2021). Whereas Zn acted as an antioxidant and detergent in lubricants, it was released into the environment as vehicle components wear out (Wang *et al*., 2020). Their spatial distribution also confirmed that high concentrations of Pb and Zn were mainly observed in urban and roadside areas (Figure 2). In addition, the ADB is rich in metallic mineral resources, and Tajikistan leads the CA region in lead- zinc ore reserves (Central Asian Geoportal; Kodirov *et al*., 2018). Therefore, F4 could be considered as traffic and mining activities.

3.4 Regional geochemical baseline of the HMs in surface sediments of the ADB

Geochemical baselines can reflect the change of surface environment, and they play a key role in managing environmental pollution (Magesh *et al*., 2021). Studies showed that the accumulated human activities in the ADB might expose the surface environment to pollution by HMs and other toxic substances (Kodirov *et al*., 2018; Zhan *et al*., 2020). Hence, it is crucial to distinguish between geochemical and anthropogenic influences in the ADB by establishing the regional GBVs. The CFD method and normalization method were the most commonly used methods for determining the regional GBVs of various elements in sediments (Lepeltier, 1969; Jiang *et al*., 2021; Magesh *et al*., 2021). In this study, both CFD method and normalization method were adopted to calculate the GBVs of the HMs in the study area and the average of the GBV for each HM calculated by the two methods was used as the final determined GBV. The CFD curves and the relationship between Al and HM concentrations were plotted in Figure S1 and Figures S2–S3, respectively. In general, the results of GBVs of HMs calculated by the CDF method were similar with those calculated by the normalized method (Table 2). The average GBVs of Cd, Zn, Pb, Cu, Ni, Cr, and Co in surface sediments of ADB were 0.27, 58.9, 14.6, 20.3, 25.8, 53.4, and 9.80 mg/kg, respectively (Table 2). In addition, the determined GBVs of Cd, Zn, Pb, Cu, Ni, Cr, and Co were also closed to the regional background values obtained from the bottom sediment cores of the Caspian Sea, Issyk-Kul and Sayram Lake, and the standard deviations were 0.04,

15.60, 5.04, 2.65, 1.99, 7.41, and 1.32, respectively. The determined GBVs were then applied to evaluate the pollution status and ecological risk of HMs.

Table 2 Geochemical baseline values established in the Amu Darya Basin and other background values (mg/kg)

HMs	M1[1]	M2[2]	M_{ave}[3]	CS[4]	LS[5]	LIK[6]
Cd	0.22	0.32	0.27	—	0.19	0.29
Zn	59.63	58.17	58.9	41.6	65.9	79.3
Pb	13.73	15.48	14.6	11.8	15.2	23.7
Cu	19.20	21.39	20.3	14.3	19.5	17.5
Ni	23.83	27.85	25.8	27.4	—	22.6
Cr	50.02	56.68	53.4	53.0	37.9	44.7
Co	9.61	10.04	9.80	11.5	—	13.0

[1] GBVs of HMs determined by the CDF method; [2] GBVs of HMs determined by the normalization method; [3] average values calculated by the two methods; [4] Caspian Sea (De Mora *et al*., 2004); [5] Lake Sayram (Zeng *et al*., 2014); [6] Lake Issyk-Kul (Wang *et al*., 2021b)

3.5 Pollution assessment of HMs

Pollution indices including *PI*, *PLI*, E^i_r and *PERI* were employed to evaluate the pollution degree of HMs in surface sediments of the ADB. The evaluation thresholds are defined by the corresponding classification criteria, see Table S2. The results showed the average *PI* values for the seven HMs in surface sediments of the ADB ranged from 1 to 3, which indicated that the whole study area was generally at a moderate level (Figure 5a). For some sample sites, however, the *PI* values of selected HMs exceeded 3, revealing a considerably even highly contaminated level. Among them, samples S93, S95, S96, S102, S104, S107, S115 and S119 were recorded as considerably contaminated levels ($3 < PI \leq 6$) for Cd, and S94 were recorded as highly contaminated levels ($PI > 6$) for Cd. Sample S108 and samples S95 and S14 were observed to be considerably contaminated levels for Zn and Pb, respectively. Sample 20 and samples S115 and S119 were exhibited high and considerable contamination levels of Cu, respectively. Besides, sample S115 was also recorded with highly contaminated levels of Cr and Ni. Spatially, Cd, Zn and Pb contamination in sediments mainly occurred near urban factories or along roads, derived from industrial discharges, vehicle exhaust and mining activities (Kodirov *et al*., 2018; Wang *et al*., 2020; Chai *et al*., 2021). For Cu, Ni and Cr, highly contaminated sediments were recorded in agricultural areas, primarily from the extensive use of agricultural fertilizers and pesticides (Luo *et al*., 2009; Chen *et al*., 2019; Xiao *et al*., 2021).The average E^i_r values for HMs in surface sediments of the ADB were below 40, indicating that the study area was generally at a low ecological risk level, but 3.9% samples of E^i_r-Cd value were higher than 80 or even 160, which were associated with considerable or high ecological risk level (Figure 5b).

PLI is a simple and comparative index, and is a useful method for examining the combined pollution levels of HMs (Tomlinson *et al*., 1980; Ramazanova *et al*., 2021). Similarly, the *PLI* values also suggested that the surface sediments in ADB were at a moderate pollution level, with 61.7% of the samples having varying degrees of contamination ($1 < PLI$) (Figure 5c). Of these samples, 2.6% (4 samples) had *PLI* values between 2–5, which were classified as high risk level, and 59.1% were categorized as moderate risk level ($1 \leq PLI \leq 2$).

Overall, 13 samples in the ADB had *PERI* values in the range of 100–200, indicating a moderate risk level; 1 sample (S94) were recorded as *PERI* values >200, showing a considered risk level; and the remaining 140 samples exhibited a low risk level (*PERI* < 100) (Figure 5d).

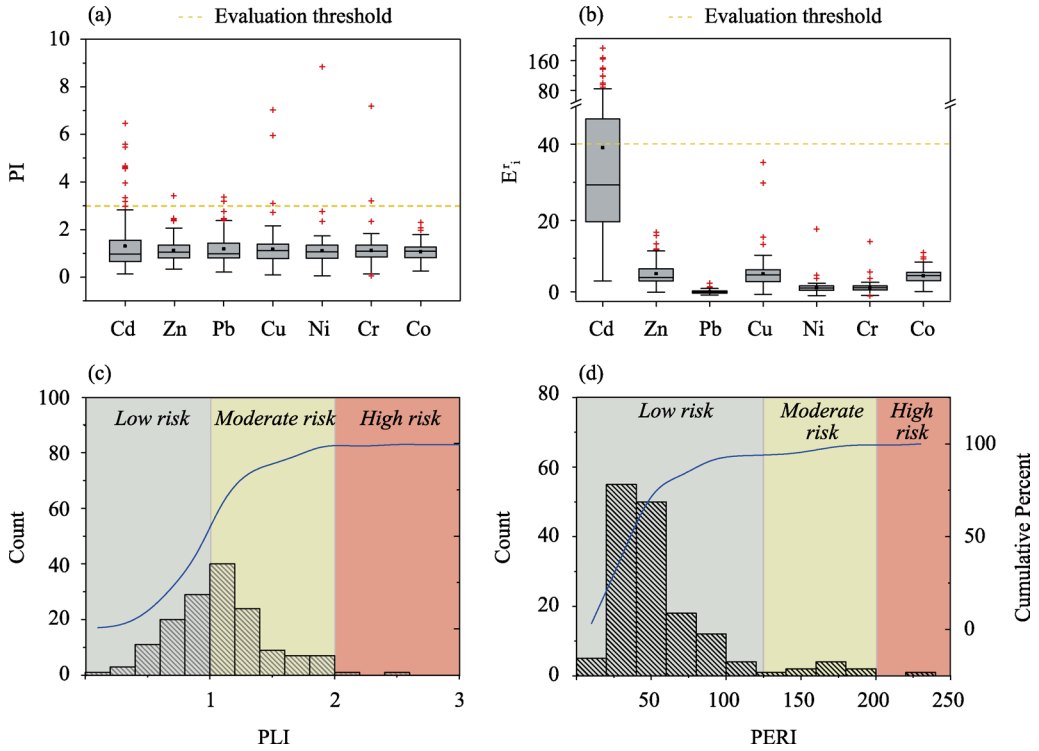

Figure 5 Boxplot of *PI* (a) and E^r_i (b) of each HM in different areas, and cumulative percentage of the sum of *PLI* (c) and *PERI* (d)

According to various indices, surface sediments of the ADB were found to be at an overall moderate pollution level of HMs and remained at a low ecological risk level. Relatively severe pollution and high risk were primarily found near urban and irrigated agricultural areas, including the municipality of Dushanbe as well as the farmlands in the lower ADB. This occurrence is in line with the fact that these areas are characterized by intensive human activities such as mining activities, industrial discharges, transport emissions and agricultural fertilizer and pesticide use (Skipperud *et al*., 2013; Zhan *et al*., 2020; Ramazanova *et al*., 2021). Hence, to preserve the ecological environment and economic development, industrial waste and vehicle emissions should be subjected to priority management in urban areas, and the use of fertilizers and pesticides in agricultural areas should be rationalized.

In addition to being influenced by human activities, HMs in surface sediments were also derived from natural sources. Previous studies suggested that high geological background of HMs may be related to their parent rock inheritance or/and secondary enrichment of HMs in the sediments (Yang *et al*., 2021). Certainly, due to its geographical location, the lower ADB was affected by an arid climate with low precipitation and high evaporation, which also probably contributed to the elevated concentrations of toxic pollutants in water and sediments (Crosa *et al*., 2006; Awan *et al*., 2011; Sun *et al*., 2019). However, our results sug-

gested that HM contamination in surface sediments of the lower ADB was light except for a few sample sites, which indicated that HM pollution might not be the major contributor to human health in the area. Therefore, in our follow-up work, we intend to carry out relevant studies on other pollutants in water and sediments of the watershed that may cause health problems.

4 Conclusion

Correlation and cluster analysis, PMF model, geostatistics and various pollution indices were employed to identify HM sources, establish GBVs and evaluate the contamination levels in surface sediments of the ADB. The mean concentrations of HMs suggested the following descending order: Zn > Cr > Ni > Cu > Pb > Co > Cd. Spatially, the accumulation of HMs was greater in the cities and agricultural area. Four source factors were apportioned by PMF model. Among them, F1 represented the natural sources (Al, Ti, Fe and Co); F2 represented industrial discharge (Cd); F3 was an agricultural source (Cu, Ni and Cr); F4 was a mixed source of traffic and mining activities (Pb and Zn); and F1 to F4 accounted for 33.5%, 11.4%, 34.2% and 20.9% of the total contribution, respectively. GBVs of Cd, Zn, Pb, Cu, Ni, Cr, and Co in surface sediments of ADB were 0.27, 58.9, 14.6, 20.3, 25.8, 53.4, and 9.80 mg/kg, respectively, closing to the regional background values from the Caspian Sea, Issyk-Kul and Sayram Lake. The *PI* and *PLI* values indicated that the surface sediments of the ADB were moderately polluted by HMs. Moreover, according to E_r^i and *EPRI* results, the ADB remained mostly at a low ecological risk level, with the largest risk being Cd. The research will better understand our cognition of the spatial differences, source, and pollution levels of HMs and design targeted strategies for HMs contamination in the ADB.

Acknowledgments

We thank the CAS Research Center for Ecology and Environment of Central Asia for assistance with this work, Huawu Wu and Haiao Zeng for field assistances.

References

Adimalla N, Chen J, Qian H, 2020. Spatial characteristics of heavy metal contamination and potential human health risk assessment of urban soils: A case study from an urban region of South India. *Ecotoxicology and Environmental Safety*, 194: 110406.

Ataniyazova O A, 2003. Health and ecological consequences of the Aral Sea crisis. The 3rd World Water Forum, Regional Cooperation in Shared Water Resources in Central Asia, Kyoto, Vol. 18.

Ataniyazova O A, Baumann R A, Liem A K D *et al*., 2001. Levels of certain metals, organochlorine pesticides and dioxins in cord blood, maternal blood, human milk and some commonly used nutrients in the surroundings of the Aral Sea (Karakalpakstan, Republic of Uzbekistan). *Acta Paediatrica*, 90(7): 801–808.

Awan U K, Ibrakhimov M, Tischbein B *et al*., 2011. Improving irrigation water operation in the lower reaches of the Amu Darya River-current status and suggestions. *Irrigation and drainage*, 60(5): 600–612.

Babow S, Meisen P, 2012. The water-energy nexus in the Amu Darya River Basin: the need for sustainable solutions to a regional problem. *Global Energy Network Institute*, http://amudaryabasin.net/sites/amudaryabasin.net/files/resources/The%20water%20energy%20nexis%20in%20the%20Amu%20Darya%20River%20Basin.pdf.

Brody M, Golub A A, Eshchanov B R, 2020. Approaches to optimize Uzbekistan's investment in irrigation technologies. *Ekonomicheskaya politika*, 15(2): 136–147.

Central Asian Geoportal. Mineral resources of the Republic of Tajikistan. http://geoportal-tj.org/index.php/ geology/deposits.

Chai L, Wang Y H, Wang X *et al*., 2021. Quantitative source apportionment of heavy metals in cultivated soil and associated model uncertainty. *Ecotoxicology and Environmental Safety*, 215: 112150.

Chen R H, Chen H Y, Song L T *et al*., 2019. Characterization and source apportionment of heavy metals in the sediments of Lake Tai (China) and its surrounding sediments. *Science of The Total Environment*, 694: 133819.

China National Environmental Monitoring Centre (CNEMC), 1990. Background Value of Soil Elements in China. Beijing: China Environmental Science Press. (in Chinese)

Crosa G, Froebrich J, Nikolayenko V, 2006. Spatial and seasonal variations in the water quality of the Amu Darya River (Central Asia). *Water Research*, 40(11): 2237–2245.

de Mora S, Sheikholeslami M R, Wyse E *et al*., 2004. An assessment of metal contamination in coastal sediments of the Caspian Sea. *Marine Pollution Bulletin*, 48(1/2): 61–77.

Gunawardena J, Ziyath A M, Egodawatta P *et al*., 2014. Mathematical relationships for metal build-up on urban road surfaces based on traffic and land use characteristics. *Chemosphere*, 99: 267–271.

Hakanson L, 1980. An ecological risk index for aquatic pollution control. A sedimentological approach. *Water Research*, 14(8): 975–1001.

Hamidov A, Helming K, Balla D, 2016. Impact of agricultural land use in Central Asia: A review. *Agronomy for Sustainable Development*, 36(1): 6.

Hossain M A, Ali N M, Islam M S *et al*., 2015. Spatial distribution and source apportionment of heavy metals in sediments of Gebeng industrial city, Malaysia. *Environmental Earth Sciences*, 73(1): 115–126.

Hu W J, Liu H L, Bao A M *et al*., 2018. Influences of environmental changes on water storage variations in Central Asia. *Journal of Geographical Sciences*, 28(7): 985–1000.

Jiang H H, Cai L M, Hu G C *et al*., 2021. An integrated exploration on health risk assessment quantification of potentially hazardous elements in sediments from the perspective of sources. *Ecotoxicology and Environmental Safety*, 208: 111489.

Jiang L L, Jiapaer G, Bao A *et al*., 2019. Monitoring the long-term desertification process and assessing the relative roles of its drivers in Central Asia. *Ecological Indicators*, 104: 195–208.

Kaneko K, Chiba M, Hashizume M *et al*., 2003. Renal tubular dysfunction in children living in the Aral Sea Region. *Archives of Disease in Childhood*, 88(11): 966–968.

Karim Z, Qureshi B A L, Mumtaz M, 2015. Geochemical baseline determination and pollution assessment of heavy metals in urban sediments of Karachi, Pakistan. *Ecological Indicators*, 48: 358–364.

Karthe D, Chalov S, Borchardt D, 2015. Water resources and their management in central Asia in the early twenty first century: status, challenges and future prospects. *Environmental Earth Sciences*, 73(2): 487–499.

Kodirov O, Kersten M, Shukurov N *et al*., 2018. Trace metal (loid) mobility in waste deposits and sediments around Chadak mining area, Uzbekistan. *Science of The Total Environment*, 622: 1658–1667.

Lepeltier C, 1969. A simplified statistical treatment of geochemical data by graphical representation. *Economic Geology*, 64(5): 538–550.

Liao X Y, Tao H, Gong X G *et al*., 2019. Exploring the database of a soil environmental survey using a geo-self-organizing map: A pilot study. *Journal of Geographical Sciences*, 29(10): 1610–1624.

Luo L, Ma Y, Zhang S *et al*., 2009. An inventory of trace element inputs to agricultural sediments in China. *Journal of Environmental Management*, 90(8): 2524–2530.

Ma L, Abuduwaili J, Li Y M *et al*., 2018. Controlling factors and pollution assessment of potentially toxic elements in topsoils of the Issyk-Kul Lake Region, Central Asia. *Soil and Sediment Contamination*: *An International Journal*, 27(2): 147–160.

Ma Y, Li Y P, Huang G H, 2020. A bi-level chance-constrained programming method for quantifying the effectiveness of water-trading to water-food-ecology nexus in Amu Darya River basin of Central Asia. *Environmental Research*, 183: 109229.

Magesh N S, Tiwari A, Botsa S M *et al*., 2021. Hazardous heavy metals in the pristine lacustrine systems of Antarctica: Insights from PMF model and ERA techniques. *Journal of Hazardous Materials*, 412: 125263.

Micklin P, 2007. The Aral Sea disaster. *Annual Review of Earth and Planetary Sciences*, 35: 47–72.

Mueller L, Suleimenov M, Karimov A *et al*., 2014. Novel measurement and assessment tools for monitoring and management of land and water resources in agricultural landscapes of Central Asia. In: Land and Water Resources of Central Asia, Their Utilisation and Ecological Status. Cham: Springer, 3–59.

Nie M L, Wen Z X, Wang Z M *et al*., 2020. Genesis and evaporative fractionation of subsalt condensate in the northeastern margin of the Amu Darya Basin. *Journal of Petroleum Science and Engineering*, 188: 106674.

Paatero P, Tapper U, 1994. Positive matrix factorization: A no-negative factor model with optimal utilization of error estimates of data values. *Environmetrics*, 5(2): 111–126.

Ramazanova E, Lee S H, Lee W, 2021. Stochastic risk assessment of urban soils contaminated by heavy metals in

Kazakhstan. *Science of The Total Environment*, 750: 141535.

Salehie O, Ismail T, Shahid S *et al*., 2021. Ranking of gridded precipitation datasets by merging compromise programming and global performance index: A case study of the Amu Darya basin. *Theoretical and Applied Climatology*, 144(3): 985–999.

Shen B B, Wu J L, Zhan S E *et al*., 2021. Spatial variations and controls on the hydrochemistry of surface waters across the Ili-Balkhash Basin, arid Central Asia. *Journal of Hydrology*, 600: 126565.

Shukurov N, Kodirov O, Peitzsch M *et al*., 2014. Coupling geochemical, mineralogical and microbiological approaches to assess the health of contaminated soil around the Almalyk mining and smelter complex, Uzbekistan. *Science of The Total Environment*, 476: 447–459.

Skipperud L, Strømman G, Yunusov M *et al*., 2013. Environmental impact assessment of radionuclide and metal contamination at the former U sites Taboshar and Digmai, Tajikistan. *Journal of Environmental Radioactivity*, 123: 50–62.

Sun J, Li Y, Suo C *et al*., 2019. Impacts of irrigation efficiency on agricultural water-land nexus system management under multiple uncertainties: A case study in Amu Darya River basin, Central Asia. *Agricultural Water Management*, 216: 76–88.

Taylor S R, 1964. Abundance of chemical elements in the continental crust: A new table. *Geochimica Et Cosmochimica Acta*, 28(8): 1273–1285.

The World Bank, 2021. All countries and economies. https://data.worldbank.org/indicator/SP.POP.TOTL.

Tomlinson D L, Wilson J G, Harris C R *et al*., 1980. Problems in the assessment of heavy-metal levels in estuaries and the formation of a pollution index. *Helgoländer Meeresuntersuchungen*, 33(1–4): 566–575.

Wang F F, Guan Q Y, Tian J *et al*., 2020. Contamination characteristics, source apportionment, and health risk assessment of heavy metals in agricultural soil in the Hexi Corridor. *Catena*, 191: 104573.

Wang J Z, Wu J L, Zhan S E *et al*., 2021a. Spatial enrichment assessment, source identification and health risks of potentially toxic elements in surface sediments, Central Asian countries. *Journal of Soils and Sediments*, 21(12): 3906–3916.

Wang J Z, Wu J L, Zhan S E *et al*., 2021b. Records of hydrological change and environmental disasters in sediments from deep Lake Issyk-Kul. *Hydrological Processes*, 35(4): e14136.

Wang X L, Luo Y, Sun L *et al*., 2016. Attribution of runoff decline in the Amu Darya River in Central Asia during 1951–2007. *Journal of Hydrometeorology*, 17(5): 1543–1560.

Wei C Y, Wen H L, 2012. Geochemical baselines of heavy metals in the sediments of two large freshwater lakes in China: Implications for contamination character and history. *Environmental Geochemistry and Health*, 34(6): 737–748.

Wu M L, Jia Y N, Zhang Y Z, 2021. Heavy metal pollution from copper smelting during the Shang Dynasty at the Laoniupo site in the Bahe River valley, Guanzhong Basin, China. *Journal of Geographical Sciences*, 31(11): 1675–1693.

Xiao H, Shahab A, Xi B D *et al*., 2021. Heavy metal pollution, ecological risk, spatial distribution, and source identification in sediments of the Lijiang River, China. *Environmental Pollution*, 269: 116189.

Yang Q, Yang Z F, Filippelli G M *et al*., 2021. Distribution and secondary enrichment of heavy metal elements in karstic sediments with high geochemical background in Guangxi, China. *Chemical Geology*, 567: 120081.

Zeng H A, Wu J L, Liu W, 2014. Two-century sedimentary record of heavy metal pollution from Lake Sayram: A deep mountain lake in central Tianshan, China. *Quaternary International*, 321: 125–131.

Zhan S E, Wu J L, Jin M, 2022. Hydrochemical characteristics, trace element sources, and health risk assessment of surface waters in the Amu Darya Basin of Uzbekistan, arid Central Asia. *Environmental Science and Pollution Research*, 29: 5269–5281.

Zhan S E, Wu J L, Wang J Z *et al*., 2020. Distribution characteristics, sources identification and risk assessment of n-alkanes and heavy metals in surface sediments, Tajikistan, Central Asia. *Science of The Total Environment*, 709: 136278.

Zhang M, Chen Y N, Shen Y J *et al*., 2019. Tracking climate change in Central Asia through temperature and precipitation extremes. *Journal of Geographical Sciences*, 29(1): 3–28.

Zhang W F, Wu J L, Zhan S E *et al*., 2021. Environmental geochemical characteristics and the provenance of sediments in the catchment of lower reach of Yarlung Tsangpo River, southeast Tibetan Plateau. *Catena*, 200: 105150.

Zhou Y, Yang X P, Zhang D G *et al*., 2021. Sedimentological and geochemical characteristics of sediments and their potential correlations to the processes of desertification along the Keriya River in the Taklamakan Desert, western China. *Geomorphology*, 375: 107560.